PCCP

PAPER

View Article Online
View Journal | View Issue

Cite this: *Phys. Chem. Chem. Phys.*, 2019, **21**, 24993

Conformational isomerizations triggered by vibrational excitation of second stretching overtones†

Cláudio M. Nunes, * Igor Reva and Rui Fausto

Received 13th September 2019,
Accepted 30th October 2019

DOI: 10.1039/c9cp05070a

rsc.li/pccp

Vibrational excitation using frequency-tunable IR laser light has been developed as a powerful tool for selective manipulation of molecular conformations. In this methodology, vibrational excitation has been typically applied to the first stretching overtones (~80 kJ mol^{-1}) but also to the fundamental modes (~40 kJ mol^{-1}). Here, we demonstrate that selective conformational isomerizations are also achieved using excitation to second stretching overtones (~120 kJ mol^{-1}). The extremely weak absorptions of the second stretching overtones of molecules isolated in low-temperature matrices were measured for the first time; here using three prototype molecules: hydroxyacetone (HA), glycolic acid (GAc) and glycolamide (GAm). Benchmarking of computed anharmonic IR spectra showed that the B3LYP/SNSD method provides the best agreement with experimental frequencies of the ν(OH), 2ν(OH) and 3ν(OH) modes for the studied molecules in argon matrices. Selective irradiation at the 3ν(OH) frequencies (9850–10 500 cm^{-1}) of HA, GAc and GAm monomers in argon matrices at 15 K successfully triggers their conformational isomerization. These results open the door to extend control over conformations separated by higher barriers and to induce other transformations not energetically accessible by excitation to the fundamental or first stretching overtone modes.

1. Introduction

In the last two decades, vibrational excitation has been applied to achieve exceptional control over molecular conformations and to generate elusive conformers otherwise inaccessible to experiments (Scheme 1).[1–4] Using frequency-tunable IR laser light, energy can be selectively deposited in a vibrationally excited state of a particular molecular structure.[5] If subsequent energy relaxation occurs by intramolecular vibrational redistribution leading to activation of a torsional mode, above the barrier, a conformational change is induced.[6] In order to suppress the following thermal conversions and allow trapping high energy conformers, low-temperature conditions provided by matrix-isolation technique are typically used. This approach has been employed to investigate molecular conformations of different families of compounds, such as carboxylic acids,[1,7–10] amino acids[11–15] and DNA bases.[16,17] Most examples involve the vibrational excitation of an OH group and conformational isomerization at the same OH or at an adjacent CC bond. Recently, it has also been demonstrated that vibrational excitation induces conformational isomerization in a remote molecular fragment, *i.e.* separated by several bonds from the group acting as an antenna. Cases were described for the flip of a remote light H atom,[18,19] and heavy hydroxymethyl (–CH_2OH),[20] methoxy (–OCH_3)[21,22] and aldehyde (–CHO)[23] fragments.

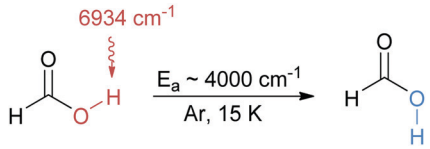

Scheme 1 Conformational isomerization induced by selective vibrational excitation as reported in seminal work by Pettersson *et al.* (1997).[1] The high energy conformer of formic acid (right) was generated by vibrational excitation of the first OH stretching overtone of the most stable form (left) in an argon matrix.

Vibrational excitation of the first overtone of an OH and NH stretching modes has been predominantly applied in this methodology, since the anharmonic transitions involving these modes have high energy [~7300–6300 cm^{-1} or ~87–75 kJ mol^{-1}] and significant enough absorption cross section. This way, conformational changes overcoming a torsional barrier up to almost 60 kJ mol^{-1} have been achieved.[10] Vibrational excitations of fundamental modes like OH, NH and CH stretching (or modes with a similar energy, ~45–30 kJ mol^{-1}) have also been applied to induce rotamerization,[24–26] but such cases are inherently constrained to lower torsional barriers and lower quantum yields.[7] To the best of our knowledge, vibrational excitation of a second stretching overtone (up to 130–120 kJ mol^{-1}) has never been considered before in this context.[27,28] Here, we

CQC, Department of Chemistry, University of Coimbra, 3004-535, Coimbra, Portugal. E-mail: cmnunes@qui.uc.pt

† Electronic supplementary information (ESI) available. See DOI: 10.1039/c9cp05070a

demonstrate that vibrational excitation to the second OH stretching overtone in three prototype molecules successfully triggers their conformational isomerization.

2. Results and discussion

Hydroxyacetone (HA), glycolic acid (GAc) and glycolamide (GAm) were selected for investigating the possibility of conformational isomerization by vibrational excitation to a second stretching overtone (Scheme 2). They are simple molecules where vibrational excitations to the first OH stretching overtone produce stable high-energy conformers under cryogenic conditions.[29–31] High-energy conformers of simple carboxylic acids such as formic and acetic acids are known to decay fast (few minutes or less) by tunneling.[1,7] Moreover, HA, GAc and GAm have strong infrared absorptions in the fundamental OH stretching and well-defined first OH stretching overtone absorptions, measured under matrix-isolation conditions, which suggests the possibility to detect experimental bands due to their second OH stretching overtones.

To the best of our knowledge there are no reports on experimental frequencies of second stretching overtones for molecules isolated under matrix-isolation conditions. The lack of such data relates with the fact that the infrared bands of higher-order overtones have extremely weak absorptions and are difficult to detect experimentally.[32,33] Intensities of the first overtone transitions are typically more than one order of magnitude weaker than those of fundamental transitions; the intensity of the next overtones is expected to progressively decrease by another order of magnitude or more.[33–35] Indeed, the first challenge in our study was to obtain such experimental data for the three case study molecules.

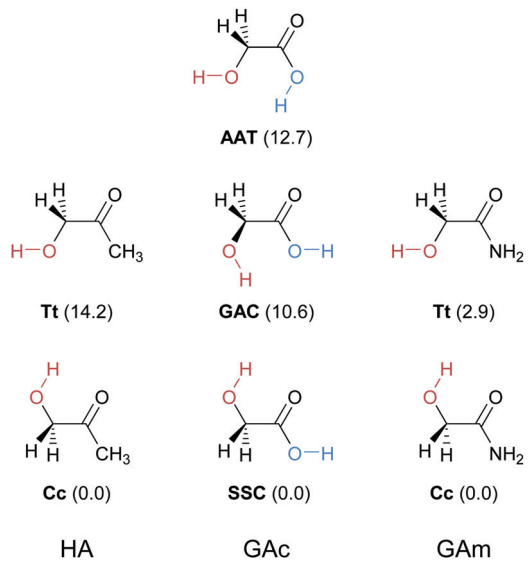

Scheme 2 Relevant conformational structures of the three selected molecules, hydroxyacetone (HA), glycolic acid (GAc) and glycolamide (GAm). The abbreviations in bold correspond to the identification of the respective conformers according to the convention adopted in previous studies.[29–31] Numbers in parentheses show the relative energies (kJ mol^{-1}, zero-point vibrational energy [ZPVE] included) calculated at the B3LYP/SNSD level of theory.

2.1. IR spectra and identification of 3ν(OH)

Monomers of HA, GAc and GAm were deposited in argon matrices at 15 K until the most intense band in the mid-IR spectrum approaches unity on the absorbance scale (Fig. S1–S3, ESI†). The spectral region where the bands due to the second OH stretching overtones [3ν(OH)] are expected to appear (10 650–9650 cm^{-1}) was then measured by accumulating approximately 8000 scans, using a thermoelectrically cooled high sensitivity InGaAs detector. HA and GAc are known to exist almost exclusively in their lowest energy conformation when isolated in an argon matrix,[29,30] which simplifies the assignments. For HA, adopting **Cc** conformation (Scheme 2), a band at 9866 cm^{-1} was observed and attributed to the 3ν(OH) mode (Fig. 1a). The bands due to 2ν(OH) and ν(OH) modes appear at 6801 and 3505 cm^{-1}, respectively. For GAc, adopting the **SSC** conformation (Scheme 2), two bands at 10 182 and 10 116 cm^{-1} were observed and attributed to the 3ν(OH)$_{acid}$ and 3ν(OH)$_{alcohol}$ modes, respectively (Fig. 2a). The bands due to 2ν(OH)$_{acid}$ and 2ν(OH)$_{alcohol}$ modes appear at 6954 and 6939 cm^{-1}, whereas absorptions due to fundamental ν(OH)$_{acid}$ and ν(OH)$_{alcohol}$ modes are overlapped, appearing both at 3561 cm^{-1}.

GAm is known to exist in two different conformations (**Cc** and **Tt**; Scheme 2) when isolated in cryogenic matrices, with both forms contributing to the mid-IR spectrum.[31] The most stable **Cc** conformation is observed with slightly larger population in the matrix and is characterized by a relatively broad ν(OH) band at 3481 cm^{-1}, whose low frequency results from an intramolecular interaction with the carbonyl group. This feature makes it very difficult to identify the corresponding band due to the second OH stretching overtone [3ν(OH)]. Nonetheless, for the **Tt** conformation a band at 10 500/10 487 cm^{-1} was clearly observed and attributed to the 3ν(OH) mode (Fig. 3a). The bands due to 2ν(OH) and ν(OH) modes of this conformer appear at 7169/7162 and 3669/3666 cm^{-1}, respectively. The observation of doublets in the OH stretching fundamental and overtone regions

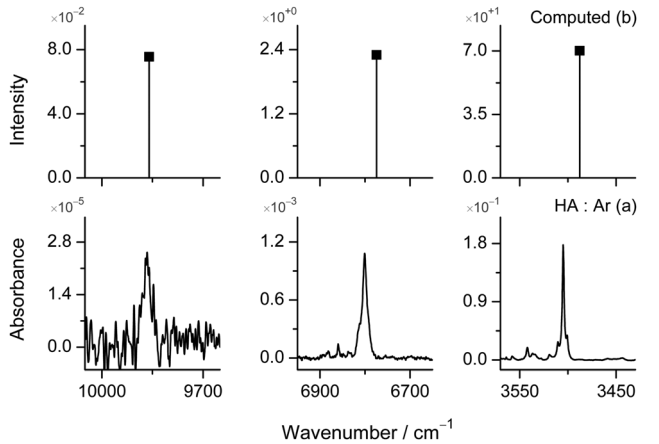

Fig. 1 (a) Experimental IR spectrum of hydroxyacetone (HA) in an argon matrix at 15 K showing absorptions corresponding to the fundamental, first and second OH stretching overtones. (b) B3LYP/SNSD computed anharmonic IR absorptions of HA (**Cc** form) corresponding to the fundamental, first and second OH stretching overtones (more details are given in the Experimental section).

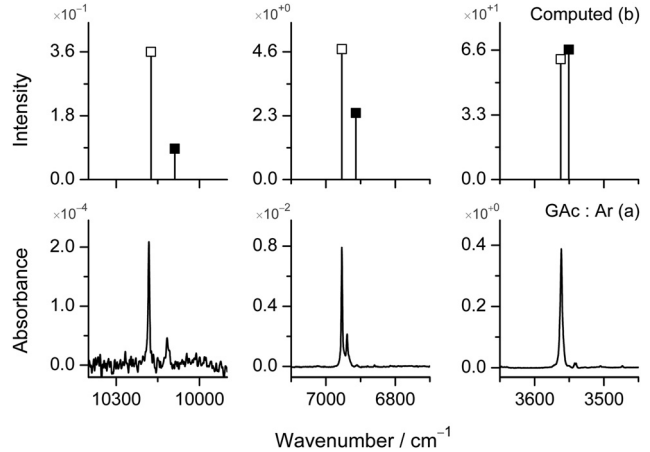

Fig. 2 (a) Experimental IR spectrum of glycolic acid (GAc) in an argon matrix at 15 K showing absorptions corresponding to the fundamental, first and second OH stretching overtones. (b) B3LYP/SNSD computed anharmonic IR absorptions of GAc (**SSC** form) corresponding to the fundamental, first and second OH stretching overtones of the acid (□) and alcohol (■) moieties.

of **Tt** is due to the existence of two different matrix environments, arguably resulting from two different argon cavities or sites surrounding the molecules.[36] This phenomenon will be shown to be relevant in the context of conformational isomerization induced by the vibrational excitations to 3ν(OH) (Section 2.3).

Anharmonic IR spectra were computed for HA, GAc and GAm (**Cc**, **SSC** and **Tt** forms, respectively) using different DFT functionals and basis sets (benchmarking of these computations is discussed in the next section). Particular attention was given for selecting the best agreement between the computed and experimental frequencies of fundamental, first and second OH stretching overtones. The best results were obtained with the B3LYP/SNSD method, which reproduces very well the experimental frequencies of the ν(OH), 2ν(OH) and 3ν(OH) modes and supports the assignment in the three studied molecules (Fig. 1–3). For instance, for HA (**Cc** form) the ν(OH), 2ν(OH) and 3ν(OH) modes were computed at 3488, 6774 and 9860 cm^{-1}, showing deviations from the corresponding experimental values equal to −17.1, −26.5 and −6.5 cm^{-1}, respectively (Fig. 1). For GAc (**SSC** form) the $\nu(\mathrm{OH})_{\mathrm{alcohol}}$, $2\nu(\mathrm{OH})_{\mathrm{alcohol}}$ and $3\nu(\mathrm{OH})_{\mathrm{alcohol}}$ modes were computed at 3551, 6913 and 10 089 cm^{-1}, showing deviations from the corresponding experimental values equal to −10.9, −25.3 and −28.0 cm^{-1}, respectively; whereas the $\nu(\mathrm{OH})_{\mathrm{acid}}$, $2\nu(\mathrm{OH})_{\mathrm{acid}}$ and $3\nu(\mathrm{OH})_{\mathrm{acid}}$ modes were computed at 3562, 6954 and 10 175 cm^{-1}, showing deviations from the corresponding experimental values equal to +0.8, −0.1 and −7.6 cm^{-1}, respectively (Fig. 2). Finally, for GAm (**Tt** form) the ν(OH), 2ν(OH) and 3ν(OH) modes were computed at 3669, 7166 and 10 491 cm^{-1}, showing deviations from the corresponding experimental values equal to +1.0, +0.6 and −2.7 cm^{-1}, respectively (Fig. 3).

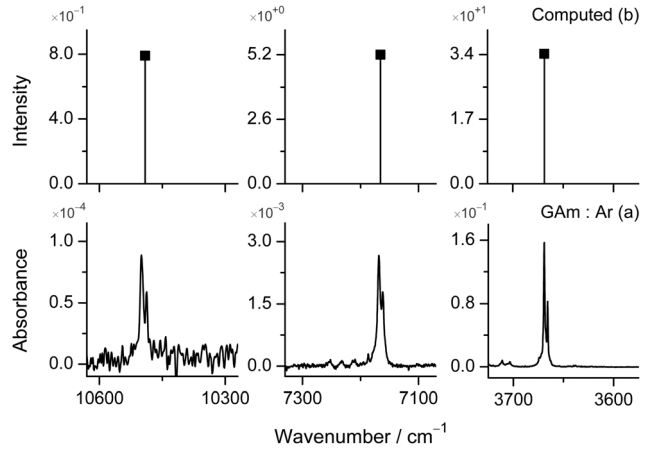

Fig. 3 (a) Experimental IR spectrum of glycolamide (GAm) in an argon matrix at 15 K showing absorptions corresponding to the fundamental, first and second OH stretching overtones of the **Tt** form. (b) B3LYP/SNSD computed anharmonic IR absorptions of GAm (the **Tt** form) corresponding to the fundamental, first and second OH stretching overtones.

2.2. Benchmarking of computed anharmonic IR spectra

Anharmonic computations of IR spectra using second-order vibrational perturbation theory (VPT2) coupled with DFT are known to show good accuracy in the description of fundamental IR modes of several medium size molecules.[37–42] Moreover, a good reproduction of overtones and combination of IR modes for some medium sized molecules has also been described,[10,23,43–45] but their systematic evaluation was only briefly addressed.[41,42,46,47] A succinct benchmarking study was carried out in this work, in the context of predicting spectral positions and supporting the identification of bands due to the second overtone stretching modes. This will be particularly relevant in the design of further experiments regarding the new methodology of chemistry triggered by vibrational excitation of second stretching overtones.

In our approach, generalized VPT2 (GVPT2) computations were used to directly obtain anharmonic vibrational frequencies of the fundamental OH stretching [ν(OH)] and the first OH stretching overtone [2ν(OH)] modes for the experimentally relevant structures of HA (**Cc** form), GAc (**SSC** form) and GAm (**Tt** form) molecules.[48] The alcohol moiety in these structures offers a single hydride oscillator which is sufficiently decoupled from other intramolecular modes.[49] The model of the anharmonic oscillator in the Morse potential was applied to analyze the OH stretching modes, assuming that they are fully localized. This model treats each OH bond as a localized Morse-like vibrator described by harmonic frequency ω_e and the Morse anharmonicity constant χ_e. The calculated values of the fundamental ν(OH) and the first overtone 2ν(OH) transitions allowed us for the determination of ω_e and χ_e. Knowing ω_e and χ_e, the anharmonic vibrational frequency of the second overtone 3ν(OH) transition was then obtained from the Morse potential.

Five different DFT functionals were tested (B2PLYP, B3LYP, B97-1, PBE0, and TPSS0) in conjugation with four basis sets (SNSD, SNST, 6-311+G(2d,p), and aug-cc-pVTZ). Some of the reasons for selecting these methods were the following: (i) standard hybrid functionals, in particular B3LYP and B97-1, in conjunction with polarised basis sets of double-ζ quality, supplemented by diffuse functions of the SNSD basis set, have been proven very satisfactory in the prediction of the anharmonic

Table 1 Anharmonic vibrational frequencies (in cm^{-1}) computed at the B3LYP/SNSD and B2PLYP/aug-cc-pVTZ levels of theory and the experimental wavenumbers (in cm^{-1}) for fundamental OH stretching, and the first and second OH stretching overtones[a]

	1ν(OH)	2ν(OH)	3ν(OH)
B3LYP/SNSD			
HA (**Cc**)	3487.8	6774.3	9859.7
GAc ($\mathbf{SSC}$)$_{alcohol}$	3550.5	6913.4	10088.5
GAc ($\mathbf{SSC}$)$_{acid}$	3562.2	6953.7	10174.6
GAm (**Tt**)	3668.6	7165.6	10491.0
B2PLYP/aug-cc-pVTZ			
HA (**Cc**)	3498.6	6800.0	9904.3
GAc ($\mathbf{SSC}$)$_{alcohol}$	3552.7	6942.9	10170.6
GAc ($\mathbf{SSC}$)$_{acid}$	3575.4	6965.1	10169.2
GAm (**Tt**)	3677.0	7186.2	10527.5
Experimental			
HA (**Cc**)	3504.9	6800.8	9866.2
GAc ($\mathbf{SSC}$)$_{alcohol}$	3561.4	6938.7	10116.5
GAc ($\mathbf{SSC}$)$_{acid}$	3561.4	6953.8	10182.2
GAm (**Tt**)$_{site\text{-}B}$	3665.9	7161.5	10487.5
GAm (**Tt**)$_{site\text{-}A}$	3669.2	7168.5	10500.0

[a] Experimental values for the band maxima were taken from infrared spectra of the matrix-isolated HA (**Cc** form), GAc (**SSC** form), and GAm (**Tt** form), see also Fig. 1–3.

Table 2 Mean absolute errors (MAEs) and maximum deviations (MAX) of anharmonic vibrational frequencies (in cm^{-1}) computed at twenty levels of theory (four DFT functionals × five basis sets) compared with experimental data[a]

Method	HA	GAc	GAm[b]	All	MAX
B2PLYP/aug-cc-pVTZ	15.1	17.6	21.5	18.1	+54.1
B2PLYP/6-311+G(2d,p)	36.2	47.2	27.7	37.0	+141.4
B2PLYP/SNST	14.5	32.8	8.8	18.7	−81.3
B2PLYP/SNSD	32.0	23.8	32.4	29.4	+68.3
B3LYP/aug-cc-pVTZ	33.2	22.9	3.9	20.0	−43.8
B3LYP/6-311+G(2d,p)	12.6	9.4	9.7	10.6	**−22.7**
B3LYP/SNST	51.3	50.2	37.9	46.4	−76.3
B3LYP/SNSD	16.7	12.1	1.4	**10.1**	−28.0
B97-1/aug-cc-pVTZ	166.1	53.6	30.1	83.3	−238.4
B97-1/6-311+G(2d,p)	45.5	36.0	60.0	47.2	+88.7
B97-1/SNST	14.3	36.6	33.3	28.1	+81.7
B97-1/SNSD	52.3	57.3	71.0	60.2	+104.9
PBE0/aug-cc-pVTZ	33.3	63.6	120.2	72.4	+183.8
PBE0/6-311+G(2d,p)	45.3	86.8	123.3	85.1	+185.9
PBE0/SNST	9.7	51.7	99.4	53.6	+151.0
PBE0/SNSD	34.3	84.5	133.6	84.1	+200.7
TPSS0/aug-cc-pVTZ	387.3	285.1	236.6	303.0	−579.3
TPSS0/6-311+G(2d,p)	370.9	271.8	220.5	287.7	−556.5
TPSS0/SNST	399.2	294.6	234.1	309.3	−597.4
TPSS0/SNSD	379.6	273.4	208.4	287.1	−568.3

[a] Experimental frequencies were obtained from the matrix-isolation infrared spectra in the regions of $n\nu$(OH) fundamental, first and second stretching overtone frequencies (n = 1, 2, and 3) for HA (**Cc** form), GAc (**SSC** form), and GAm (**Tt** form). [b] For the estimation of MAE and MAX for the **Tt** form, the experimental $n\nu$(OH) values were the average of wavenumbers between the pairs of band peaks (n = 1, 2, and 3) in site-A and site-B.

wavenumbers of fundamental vibrations for small-to-medium molecules;[42] (ii) very accurate structures and satisfactory anharmonic wavenumbers of fundamental vibrations for small-to-medium molecules were obtained also at the PBE0/SNSD level;[41,42] and (iii) for strongly anharmonic modes (but not limited to these), improved results (relatively to B3LYP) were reported to be obtained with anharmonic corrections computed at the B2PLYP/aug-cc-pVTZ level.[40,42]

A summary of the vibrational frequencies of the ν(OH) and 2ν(OH) stretching modes obtained using direct VPT2 anharmonic computations at the B3LYP/SNSD and B2PLYP/aug-cc-pVTZ levels and wavenumbers of the 3ν(OH) modes obtained from the Morse potential are shown in Table 1, together with the corresponding experimental values. A full set of the anharmonic computations is provided in the ESI† (Table S1). The benchmarking results for twenty levels of theory are shown in Table 2.

The three columns in Table 2, entitled as HA, GAc, and GAm, represent the mean absolute error (MAE) values for all OH moieties in each reference structure (**Cc** for AH; both $\mathbf{SSC}_{acid}$ and $\mathbf{SSC}_{alcohol}$ for GAc; and **Tt** for GAm) obtained as average deviation for all computed $n\nu$(OH) modes (n = 1, 2, and 3). The values in column ''All'' represent the average of the three preceding columns. The values in column MAX represent the highest deviation for an individual value over all sets of data. The best overall performance among all methods belongs to B3LYP/SNSD, with an average MAE of 10.1 cm^{-1}. It is closely followed by B3LYP/6-311+G(2d,p), with an average MAE of 10.6 cm^{-1} and the best MAX (−22.7 cm^{-1}). The B2PLYP methods represent the second-best group, yielding average MAEs between 18 and 37 cm^{-1}, where the TPSS0 method produces the least accurate data.

Overall, the results indicate that B3LYP/SNSD computed IR anharmonic frequencies provided an accurate description of OH stretching fundamental, first and second overtones for the studied molecules in argon matrices. Interestingly, the B3LYP/SNSD method provided here slightly better results than the B2PLYP/aug-cc-pVTZ method. Computations at the B2PLYP level are much more expensive than at B3LYP, because of the inclusion of second-order perturbation treatment of the electron correlation and larger basis set requirements, but they have been described as one of the most reliable ways to obtain IR anharmonic frequencies of medium size molecules.[42] In the context of matrix isolated molecules, and in particular for estimation of fundamental and overtones of OH stretching modes, the B3LYP/SNSD method appears as the best choice,[50] and due to the low computational cost and good accuracy, it is recommended to be adopted for other medium-to-large molecules.

2.3. Vibrational excitation of 3ν(OH)

Monomers of HA, GAc and GAm isolated in argon matrices were irradiated at the frequencies of their second OH stretching overtones [3ν(OH)] using tunable narrowband near-IR light (provided by a diode laser or an optical parametric oscillator pumped by a pulsed laser). To the best of our knowledge, vibrational excitation to the second stretching overtones has never been used before to manipulate molecules under matrix isolation conditions. The 3ν(OH) bands of the studied molecules were successfully measured, as described in Section 2.1. However, it was not clear *a*

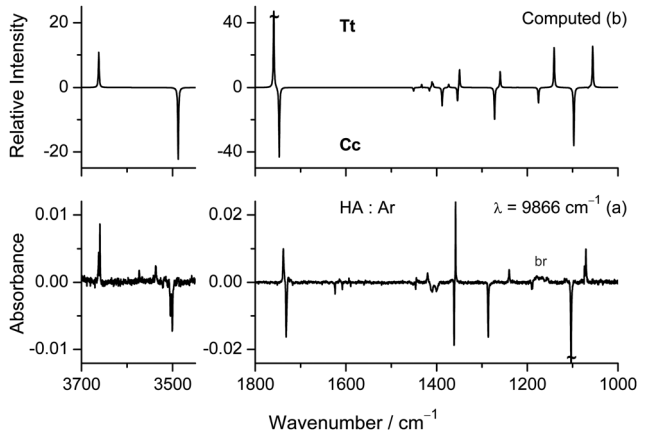

Fig. 4 (a) Experimental difference mid-IR spectrum showing changes after irradiation of hydroxyacetone (HA) in an argon matrix (15 K) at the frequency of the second O–H stretching overtone of the **Cc** form (λ = 9866 cm^{-1}). A broad experimental band of the **Tt** form growing near 1170 cm^{-1} is indicated with the label "br". (b) B3LYP/SNSD computed anharmonic difference mid-IR spectrum considering quantitative transformation of the **Cc** form (intensities multiplied by −1) into the **Tt** form of HA.

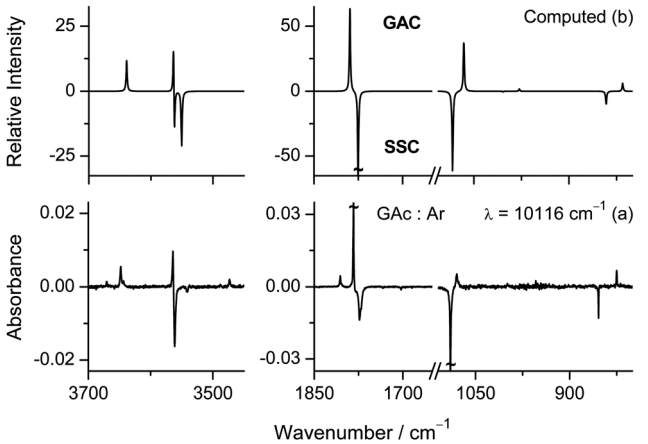

Fig. 5 (a) Experimental difference mid-IR spectrum showing changes after irradiation of glycolic acid (GAc) in an argon matrix (15 K) at the frequency of the second O–H stretching overtone of the alcohol moiety of the **SSC** form (λ = 10 116 cm^{-1}). (b) B3LYP/SNSD computed anharmonic difference mid-IR spectrum considering quantitative transformation of the **SSC** form (intensities multiplied by −1) into the **GAC** form of GAc.

priori whether pumping these modes, with small absorption cross section, would result in any transformation.

HA existing exclusively in the **Cc** conformation in a freshly deposited argon matrix was vibrationally excited at the 3ν(OH) frequency by irradiation at 9866 cm^{-1} (1013.58 nm). Monitoring the effects with mid-IR spectroscopy reveals the decrease of the bands due to the **Cc** form and the appearance of new bands due to the high-energy **Tt** form. The experimental difference IR spectrum (spectrum after irradiation "minus" that before irradiation, Fig. 4a) compares well with B3LYP/SNSD computed IR spectrum considering the **Cc** → **Tt** transformation (Fig. 4b). Particularly characteristic are the consumed bands of **Cc** at 3505, 1731 and 1103 cm^{-1}, comparing well with the corresponding computed bands at 3488 [ν(O–H)], 1747 [ν(C═O)] and 1097 [ν(C–O)] cm^{-1}; and the generated bands of **Tt** at 3661, 1738 and 1074/1071 cm^{-1}, matching well with the corresponding computed bands at 3662 [ν(O–H)], 1759 [ν(C═O)] and 1061 [ν(C–O)] cm^{-1}. The assignment of **Cc** and **Tt** also agrees with previous identification of these forms isolated in an argon matrix,[29] as presented in Tables S2 and S3 (ESI†). The results unambiguously demonstrate that irradiation of the HA **Cc** form at the 3ν(OH) frequency triggers conformational isomerization to the **Tt** form.

GAc adopting the **SSC** conformation in an argon matrix was vibrationally excited at the $3\nu(OH)_{alcohol}$ and $3\nu(OH)_{acid}$ frequencies by irradiation at 10 116 cm^{-1} (988.53 nm) and 10 182 cm^{-1} (982.13 nm), respectively. The difference mid-IR spectrum resulting from irradiation at $3\nu(OH)_{alcohol}$ reveals that **SSC** converts almost exclusively to the high-energy conformer **GAC**, as shown by the good correspondence between the experimental and the B3LYP/SNSD computed IR spectra, the latter considering the **SSC** → **GAC** transformation (Fig. 5). Particularly indicative are the consumed bands of **SSC** at 3561 and 1773 cm^{-1}, reproduced well by the corresponding computed bands at 3562/3551 [$\nu(O–H)_{acid}$/$\nu(O–H)_{alcohol}$] and 1775 cm^{-1} [ν(C═O)], and the produced bands of **GAC** at 3648, 3564 and 1783 cm^{-1}, fitted well by the corresponding computed bands at 3639 [$\nu(O–H)_{acid}$], 3563 [$\nu(O–H)_{alcohol}$] and 1789 cm^{-1} [ν(C═O)]. The identification of **SSC** and **GAC** forms also concurs with previous assignments,[30,51,52] as presented in more detail in Tables S4 and S5 (ESI†). The irradiation at $3\nu(OH)_{acid}$ (10 182 cm^{-1}) also converts **SSC**, but in this case the formation of **GAC** is accompanied by a significant amount of other high energy conformers.[53] The latter was straightforward identified as the **AAT** form based on the observed IR bands at 3670, 3473 and 1806 cm^{-1}, which are in good agreement with the corresponding B3LYP/SNSD computed bands at 3667 [$\nu(O–H)_{acid}$], 3478 [$\nu(O–H)_{alcohol}$] and 1823 cm^{-1} [ν(C═O)] (Fig. S4, ESI†), and match with the most characteristic IR bands described for this form previously generated in argon matrices.[30,51] Overall, the data clearly show that irradiation of GAc at both $3\nu(OH)_{alcohol}$ and $3\nu(OH)_{acid}$ frequencies of the **SSC** form lead to conformational isomerization to the **GAC** form (the latter irradiation also to a minor amount of the **AAT** form).

Finally, the **Tt** conformer of GAm in the argon matrix was vibrationally excited at the 3ν(OH) frequency. As shown before, the **Tt** form exists in two different matrix environments, designated here as site-A and site-B, with slightly different IR signatures. This is particularly noticeable in the fundamental, first and second O–H stretching overtone ranges where $\Delta\nu$([site-A]–[site-B]) is ~3, 7 and 13 cm^{-1}, respectively (see Table 1). Both irradiation at 10 500 and 10 487 cm^{-1} (952.38 and 953.56 nm), corresponding to the experimental 3ν(OH) absorption band of **Tt** in site-A and site-B, respectively, leads to the consumption of **Tt** and the production of the **Cc** conformer (Fig. S5, ESI†). The identification of **Tt** and **Cc** conformers of GAm is unequivocal, not only due to the excellent agreement between the experimental and computed IR spectra but also based on the comparison with previous data for these two conformers isolated in argon matrices[31] (Tables S6 and S7, ESI†). Interestingly, we found that the **Tt** → **Cc** conformational

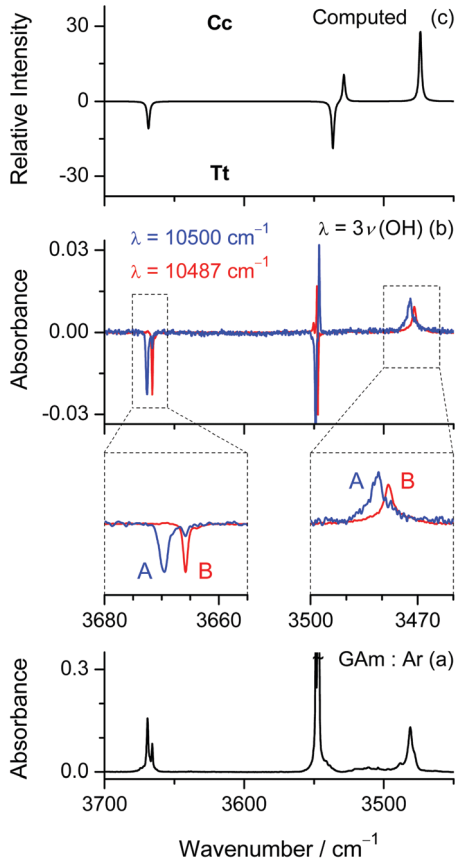

Fig. 6 (a) Selected region of the experimental mid-IR spectrum of glycolamide (GAm) in an argon matrix (15 K) showing absorptions corresponding to the fundamental OH stretching modes of **Tt** and **Cc** forms. (b) Experimental difference mid-IR spectra showing changes after irradiation of the **Tt** form in an argon matrix (15 K) at the frequency of the second OH stretching overtone, for molecules packed in two different matrix sites: λ = 10 500 (A, blue) and 10 487 cm^{-1} (B, red). Note that difference mid-IR after irradiation at 10 500 cm^{-1} was multiplied by a factor of 3 to normalize the peak intensity for the ν(OH) band due to the consumed **Tt** form. (c) B3LYP/SNSD computed anharmonic difference mid-IR spectrum considering quantitative transformation of the **Tt** form (intensities multiplied by −1) into the **Cc** form of GAm.

isomerization induced upon excitation at the second OH stretching overtone is site-selective. This means that the manipulation of a specific molecular conformer can be controlled at its environmental level.[36,54] For instance, irradiation at 10 500 cm^{-1} (952.38 nm) leads to the consumption of **Tt** in site-A, whereas irradiation at 10 487 cm^{-1} (953.56 nm) consumes **Tt** in site-B (Fig. 6). This is demonstrated by the selective depletion of the ν(OH) band of **Tt** at 3669.2 and 3665.9 cm^{-1} and the formation of the ν(OH) bands of **Cc** at 3481.0 and 3478.2 cm^{-1}, respectively. A more detailed characterization of the IR spectra of **Tt** and **Cc** conformers at the two different sites is given in Tables S6 and S7 (ESI†).

3. Conclusions

In summary, we measured for the first time the extremely weak absorptions of second stretching overtones in monomeric molecules isolated in low-temperature matrices (argon at 15 K),

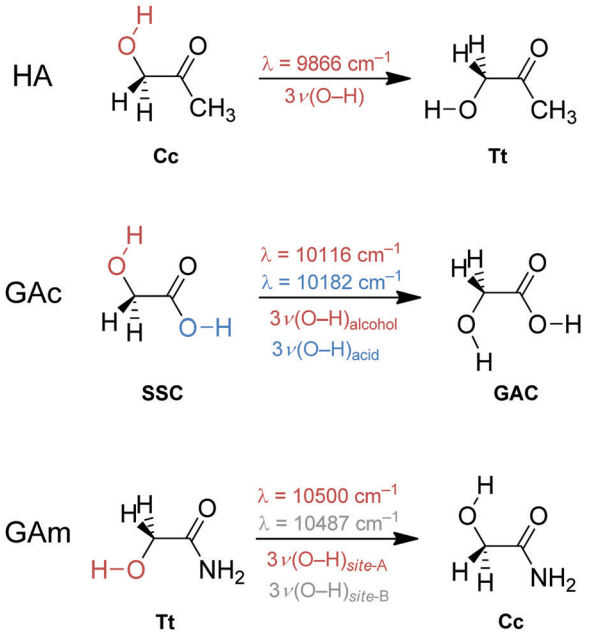

Scheme 3 Summary of the results of conformational isomerizations triggered by vibrational excitation of the second OH stretching overtones (*i.e.*, 3ν(OH) modes) in the three prototype molecules, hydroxyacetone (HA), glycolic acid (GAc) and glycolamide (GAm).

namely the 3ν(OH) modes in three prototype species: hydroxyacetone (HA), glycolic acid (GAc) and glycolamide (GAm). Benchmarking of computed anharmonic IR spectra using five different DFT functionals (B2PLYP, B3LYP, B97-1, PBE0, and TPSS0) in conjugation with four basis sets (SNSD, SNST, 6-311+G(2d,p), and aug-cc-pVTZ) showed that the B3LYP/SNSD method provides the best agreement with experimental frequencies of the ν(OH), 2ν(OH) and 3ν(OH) modes for the studied molecules (an average mean absolute error of 10.1 cm^{-1}). Finally, using frequency-tunable IR laser light, we demonstrate that selective vibrational excitation to the second OH stretching overtones in the three prototype molecules successfully triggers their conformational isomerizations (Scheme 3). Vibrational excitation applied to the first stretching overtones, or less frequently to fundamental modes, in conjugation with low-temperature conditions, has been developed as a powerful tool to control molecular conformations. The inaugural results presented here with vibrational excitation to the second stretching overtones open the door for new opportunities in controlling chemical transformations not energetically accessible by excitation to the fundamental or first stretching overtone modes.

4. Experimental and computational methods

4.1. Samples

Commercial samples of hydroxyacetone (Alfa Aesar, purity 95%), glycolic acid (TCI Europe, 98%) and glycolamide (Sigma-Aldrich, 98%) were used.

4.2. Matrix isolation

To prepare low-temperature matrices of hydroxyacetone and glycolic acid, a sample was placed into a glass tube connected to the vacuum chamber of a cryostat through a stainless steel needle valve. In the case of glycolamide, the solid compound was placed in a miniature glass oven attached to the vacuum chamber of a cryostat. Prior to deposition, all the samples were purified from the volatile impurities by pumping through the cryostat at room temperature. A CsI window, used as an optical substrate, was cooled to 15 K using a closed-cycle helium refrigerator (APD Cryogenics, with a DE-202A expander), equipped with polished potassium bromide (KBr) outer windows, and under a pressure of approximately 10^{-6} mbar. The temperature was measured directly at the sample holder, by using a silicon diode sensor connected to a digital controller (Scientific Instruments, Model 9650-1). Then sample vapours were co-deposited with an excess of argon (Air Liquide, purity 99.9999%). Hydroxyacetone vapours were produced by keeping the sample tube immersed in a water/ethanol bath at −40 °C. Glycolic acid vapours were produced by keeping the sample tube at room temperature immersed in a water bath at 20 °C. Glycolamide vapours were produced by heating the compound at 70 °C in the miniature glass oven. The process of matrix deposition took approximately 2 hours and was controlled by recording IR spectra.

4.3. IR spectroscopy

The IR spectra of the matrix isolated samples were recorded with a Thermo Nicolet 6700 Fourier transform infrared spectrometer. In the mid-IR region (4000–400 cm^{-1}) the spectra were recorded with 0.5 cm^{-1} resolution (with typically a total of 128 scans) using a deuterated triglycine sulphate (DTGS) detector, a KBr beamsplitter and an ETC EverGlo globar source. In the near-IR region corresponding to the first OH stretching overtone modes (7500–6500 cm^{-1}) the spectra were recorded with 2 cm^{-1} resolution (with typically a total of 256 scans), whereas in the near-IR region corresponding to the second OH stretching overtone modes (10 650–9650 cm^{-1}) the spectra were recorded with 4 cm^{-1} resolution (with typically a total of 8000 scans), in both cases using a thermoelectrically cooled indium gallium arsenide (InGaAs) detector, a CaF_2 beamsplitter and a Whitelight globar source. To avoid interference from atmospheric H_2O and CO_2, a stream of dry air was continuously purged through the optical path of the spectrometer.

4.4. Near-IR irradiation

The matrix-isolated samples were irradiated at the frequency of the second OH stretching overtones using two monochromatic near-IR light sources: (i) tunable near-IR light (full range) generated as the idler beam of a Spectra Physics Quanta-Ray MOPO-SL optical parametric oscillator (fwhm 0.2 cm^{-1}, pulse energy 10 mJ), pumped with a pulsed Nd:YAG laser (10 ns, repetition rate 10 Hz), and (ii) tunable near-IR light ($\sim$10 500–10 100 cm^{-1}) generated by a continuous wave diode laser Toptica DLC TA PRO (fwhm $<$1 MHz, up to 3 W). In a typical experiment, irradiation was carried out for 20 min using 120 mW of power. Similar results were obtained using both near-IR light sources.

4.5. IR spectra computations

To support the analysis of the experimental IR spectra, geometry optimizations and anharmonic frequency computations were performed at the B3LYP/SNSD level of theory using Gaussian 16 (Revision B.01).[55] Anharmonic IR spectra were computed using generalized second-order vibrational perturbation theory (GVPT2)[56,57] as implemented in Gaussian 16. This approach enables the evaluation of fundamental, overtone and combination bands (up to two quanta) and their corresponding infrared intensities. The second OH stretching overtone frequency was calculated considering a Morse potential with an anharmonicity constant estimated from the frequencies computed for the fundamental OH stretching mode and the first OH stretching overtone. The infrared intensity of the 3ν(OH) mode was roughly estimated as the computed intensity of 2ν(OH) multiplied by the ratio of the intensities of ν(OH) and 2ν(OH).

For comparing the computed and experimental mid-IR spectra, the calculated anharmonic frequencies of fundamental modes and the respective intensities were convoluted with Lorentzian functions having an fwhm of 2 cm^{-1}, centered at the calculated anharmonic frequency. The integrated area of each simulated peak was set to be equal to the computed IR intensity (in km mol^{-1}). Assignments of vibrational modes were made by inspection of ChemCraft animations.[58]

4.6. Benchmarking of computed anharmonic IR spectra

Benchmarking of DFT methods in computations of anharmonic IR frequencies was carried out to assess the frequencies of the fundamental, first and second OH stretching overtones of hydroxyacetone, glycolic acid and glycolamide molecules (**Cc**, **SSC**, and **Tt** forms, respectively). All calculations were performed with very tight optimization criteria, superfine integration grid and following the procedure described in the ''IR Spectra Computations'' section. Five different DFT functionals were tested: the B2PLYP[59] double-hybrid-GGA; the B3LYP,[60,61] B97-1,[62] and PBE0[63] hybrid-GGA; and the TPSS0[62] hybrid meta-GGA. In conjugation with these functionals, four different basis sets were used: the double-ζ SNSD and triple-ζ SNST basis sets developed by Barone *et al.*;[64,65] the Pople type[66] 6-311+G(2d,p) basis set; and the Dunning type[67] aug-cc-pVTZ basis set. Exploratory calculations using Grimme dispersion correction (D3) in combination with Becke–Johnson (BJ) damping[68] were performed but no significantly different results were obtained. The computed results were then compared with the experimental IR frequencies of the molecules isolated in argon matrices at 15 K.

Author contributions

C. M. N. conceived the original working hypothesis, performed the experiments and conducted computations. C. M. N. and I. R. analysed the data. All authors co-wrote the manuscript.

Conflicts of interest

There are no conflicts to declare.

Acknowledgements

This work was supported by the Project POCI-01-0145-FEDER-028973, funded by FEDER *via* Portugal 2020 – POCI, and by National Funds *via* the Portuguese Foundation for Science and Technology (FCT). The Coimbra Chemistry Centre is supported by the FCT through the project UID/QUI/0313/2019, co-funded by COMPETE. C. M. N. and I. R. acknowledge the FCT for an Auxiliary Researcher grant and an Investigador FCT grant, respectively. Gil Ferreira is acknowledged for the assistance in the experiments performed with glycolamide.

Notes and references

1 M. Pettersson, J. Lundell, L. Khriachtchev and M. Räsänen, *J. Am. Chem. Soc.*, 1997, **119**, 11715–11716.
2 B. C. Dian, A. Longarte and T. S. Zwier, *Science*, 2002, **296**, 2369–2373.
3 A. J. Lopes Jesus, C. M. Nunes, I. Reva, S. M. V. Pinto and R. Fausto, *J. Phys. Chem. A*, 2019, **123**, 4396–4405.
4 R. Fausto, L. Khriachtchev and P. Hamm, in *Physics and Chemistry at Low Temperatures*, ed. L. Khriachtchev, Pan Stanford Publishing, USA, 2011, pp. 51–84.
5 E. M. S. Maçôas, L. Khriachtchev, M. Pettersson, J. Juselius, R. Fausto and M. Räsänen, *J. Chem. Phys.*, 2003, **119**, 11765–11772.
6 R. Schanz, V. Boţan and P. Hamm, *J. Chem. Phys.*, 2005, **122**, 044509.
7 E. M. S. Maçôas, L. Khriachtchev, M. Pettersson, R. Fausto and M. Räsänen, *J. Am. Chem. Soc.*, 2003, **125**, 16188–16189.
8 E. M. S. Maçôas, L. Khriachtchev, M. Pettersson, R. Fausto and M. Räsänen, *J. Phys. Chem. A*, 2005, **109**, 3617–3625.
9 L. Lapinski, I. Reva, H. Rostkowska, A. Halasa, R. Fausto and M. J. Nowak, *J. Phys. Chem. A*, 2013, **117**, 5251–5259.
10 I. Reva, C. M. Nunes, M. Biczysko and R. Fausto, *J. Phys. Chem. A*, 2015, **119**, 2614–2627.
11 G. Bazsó, G. Magyarfalvi and G. Tarczay, *J. Phys. Chem. A*, 2012, **116**, 10539–10547.
12 C. M. Nunes, L. Lapinski, R. Fausto and I. Reva, *J. Chem. Phys.*, 2013, **138**, 125101.
13 G. Bazsó, E. E. Najbauer, G. Magyarfalvi and G. Tarczay, *J. Phys. Chem. A*, 2013, **117**, 1952–1962.
14 E. E. Najbauer, G. Bazsó, S. Góbi, G. Magyarfalvi and G. Tarczay, *J. Phys. Chem. B*, 2014, **118**, 2093–2103.
15 E. E. Najbauer, G. Bazsó, R. Apóstolo, R. Fausto, M. Biczysko, V. Barone and G. Tarczay, *J. Phys. Chem. B*, 2015, **119**, 10496–10510.
16 L. Lapinski, M. J. Nowak, I. Reva, H. Rostkowska and R. Fausto, *Phys. Chem. Chem. Phys.*, 2010, **12**, 9615–9618.
17 L. Lapinski, I. Reva, H. Rostkowska, R. Fausto and M. J. Nowak, *J. Phys. Chem. B*, 2014, **118**, 2831–2841.
18 A. Halasa, L. Lapinski, H. Rostkowska and M. J. Nowak, *J. Phys. Chem. A*, 2015, **119**, 9262–9271.
19 B. Kovács, N. Kuş, G. Tarczay and R. Fausto, *J. Phys. Chem. A*, 2017, **121**, 3392–3400.
20 A. Halasa, I. Reva, L. Lapinski, H. Rostkowska, R. Fausto and M. J. Nowak, *J. Phys. Chem. A*, 2016, **120**, 2647–2656.
21 A. J. Lopes Jesus, I. Reva, C. Araujo-Andrade and R. Fausto, *J. Am. Chem. Soc.*, 2015, **137**, 14240–14243.
22 A. J. Lopes Jesus, R. Fausto and I. Reva, *J. Phys. Chem. A*, 2017, **121**, 3372–3382.
23 A. J. Lopes Jesus, C. M. Nunes, R. Fausto and I. Reva, *Chem. Commun.*, 2018, **54**, 4778–4781.
24 T. N. Wassermann, M. A. Suhm, P. Roubin and S. Coussan, *J. Mol. Struct.*, 2012, **1025**, 20–32.
25 S. Coussan and G. Tarczay, *Chem. Phys. Lett.*, 2016, **644**, 189–194.
26 F. Duvernay, T. Butscher, T. Chiavassa and S. Coussan, *Chem. Phys.*, 2017, **496**, 9–14.
27 Two examples are known of chemistry induced by vibrational excitation of a second stretching overtone in gas-phase: the dissociation of peroxynitric acid and hydroxymethyl radical upon exciation to their OH stretching second overtone (ref. 27*a* and *b*). Note that vibrational excitations to higher stretching overtones are also known to iniciate unimolecular reactions is several molecules with relevance for atmospheric chemistry (ref. 27*c*). (*a*) C. M. Roehl, S. A. Nizkorodov, H. Zhang, G. A. Blake and P. O. Wennberg, *J. Phys. Chem. A*, 2002, **106**, 3766–3772; (*b*) J. Wei, B. Karpichev and H. Reisler, *J. Chem. Phys.*, 2006, **125**, 034303; (*c*) V. Vaida and D. J. Donaldson, *Phys. Chem. Chem. Phys.*, 2014, **16**, 827–836.
28 It has been claimed that in matrix isolation conditions, conformational isomerizations can be induced by high-overtone excitation with visible light (532 nm) from a Raman laser source (ref. 28*a–c*). (*a*) A. Olbert-Majkut, J. Ahokas, J. Lundell and M. Pettersson, *J. Chem. Phys.*, 2008, **129**, 041101; (*b*) A. Olbert-Majkut, J. Ahokas, M. Pettersson and J. Lundell, *J. Phys. Chem. A*, 2013, **117**, 1492–1502; (*c*) J. M. E. Ahokas, I. Kosendiak, J. Krupa, M. Wierzejewska and J. Lundell, *J. Raman Spectrosc.*, 2018, **49**, 2036–2045.
29 A. Sharma, I. Reva and R. Fausto, *J. Am. Chem. Soc.*, 2009, **131**, 8752–8753.
30 A. Halasa, L. Lapinski, I. Reva, H. Rostkowska, R. Fausto and M. J. Nowak, *J. Phys. Chem. A*, 2014, **118**, 5626–5635.
31 L. Lapinski, I. Reva, H. Rostkowska, A. J. Lopes Jesus, S. M. Vieira Pinto, R. Fausto and M. J. Nowak, *J. Phys. Chem. A*, 2019, **123**, 3831–3839.
32 D. K. Havey, K. J. Feierabend and V. Vaida, *J. Phys. Chem. A*, 2004, **108**, 9069–9073.
33 D. K. Havey, K. J. Feierabend, K. Takahashi, R. T. Skodje and V. Vaida, *J. Phys. Chem. A*, 2006, **110**, 6439–6446.
34 K. Takahashi, K. L. Plath, R. T. Skodje and V. Vaida, *J. Phys. Chem. A*, 2008, **112**, 7321–7331.
35 K. L. Plath, K. Takahashi, R. T. Skodje and V. Vaida, *J. Phys. Chem. A*, 2009, **113**, 7294–7303.
36 E. M. S. Maçôas, L. Khriachtchev, M. Pettersson, J. Lundell, R. Fausto and M. Räsänen, *Vib. Spectrosc.*, 2004, **34**, 73–82.

37 C. Puzzarini, J. Bloino, N. Tasinato and V. Barone, *Chem. Rev.*, 2019, **119**, 8131–8191.
38 V. Barone, *Wiley Interdiscip. Rev.: Comput. Mol. Sci.*, 2016, **6**, 86–110.
39 J. Bloino, M. Biczysko and V. Barone, *J. Chem. Theory Comput.*, 2012, **8**, 1015–1036.
40 M. Biczysko, P. Panek, G. Scalmani, J. Bloino and V. Barone, *J. Chem. Theory Comput.*, 2010, **6**, 2115–2125.
41 J. Bloino, A. Baiardi and M. Biczysko, *Int. J. Quantum Chem.*, 2016, **116**, 1543–1574.
42 V. Barone, M. Biczysko and J. Bloino, *Phys. Chem. Chem. Phys.*, 2014, **16**, 1759–1787.
43 K. A. E. Meyer and M. A. Suhm, *Chem. Sci.*, 2019, **10**, 6285–6294.
44 J. Grabska, K. B. Beć, Y. Ozaki and C. W. Huck, *J. Phys. Chem. A*, 2017, **121**, 1950–1961.
45 K. B. Beć, Y. Futami, M. J. Wójcik, T. Nakajima and Y. Ozaki, *J. Phys. Chem. A*, 2016, **120**, 6170–6183.
46 V. Barone, M. Biczysko, J. Bloino, P. Cimino, E. Penocchio and C. Puzzarini, *J. Chem. Theory Comput.*, 2015, **11**, 4342–4363.
47 J. Bloino, *J. Phys. Chem. A*, 2015, **119**, 5269–5287.
48 In the process, anharmonic computations also provided information for all remaining fundamental modes, overtones, and combination transitions up to two quanta, including their infrared intensities. Indeed, B3LYP/SNSD computed anharmonic IR fundamental modes were used to assist the assignment of the transformations induced in the three prototype molecules (HA, GAc and GAm) decribed in Section 2.3.
49 F. Kollipost, K. Papendorf, Y. F. Lee, Y. P. Lee and M. A. Suhm, *Phys. Chem. Chem. Phys.*, 2014, **16**, 15948–15956.
50 The better agreement with the matrix infrared spectroscopy data does not necessarily mean a better quality of the computational method. It is well-known that the matrix environment introduces some frequency shifts in the IR band positions compared to the gas phase (see for instance ref. 43, 46 and 50*a*). (*a*) W. Chin, M. Chevalier, R. Thon, R. Pollet, J. Ceponkus and C. Crépin, *J. Chem. Phys.*, 2004, **140**, 224319.
51 I. D. Reva, S. Jarmelo, L. Lapinski and R. Fausto, *Chem. Phys. Lett.*, 2004, **389**, 68–74.
52 I. D. Reva, S. Jarmelo, L. Lapinski and R. Fausto, *J. Phys. Chem. A*, 2004, **108**, 6982–6989.
53 It is known that the $2\nu(OH)_{acid}$ modes of **SSC** and **GAC** overlap, and therefore, irradiation of **SSC** at the $2\nu(OH)_{acid}$ frequency leads not only to excitation of the initially present form but also to excitation of the photogenerated **GAC** conformer, which subsquently results in the formation of the **AAT** conformer.[30] It is likely that a similar situation occurs during the irradiation of **SSC** at the $3\nu(OH)_{acid}$ frequency, justifying in this way the generation of **GAC** accompanied by a small amount of **AAT**.
54 L. Khriachtchev, J. Lundell, E. Isoniemi and M. Räsänen, *J. Chem. Phys.*, 2000, **113**, 4265–4273.
55 M. J. Frisch, G. W. Trucks, H. B. Schlegel, G. E. Scuseria, M. A. Robb, J. R. Cheeseman, G. Scalmani, V. Barone, G. A. Petersson, H. Nakatsuji, X. Li, M. Caricato, A. V. Marenich, J. Bloino, B. G. Janesko, R. Gomperts, B. Mennucci, H. P. Hratchian, J. V. Ortiz, A. F. Izmaylov, J. L. Sonnenberg, D. Williams-Young, F. Ding, F. Lipparini, F. Egidi, J. Goings, B. Peng, A. Petrone, T. Henderson, D. Ranasinghe, V. G. Zakrzewski, J. Gao, N. Rega, G. Zheng, W. Liang, M. Hada, M. Ehara, K. Toyota, R. Fukuda, J. Hasegawa, M. Ishida, T. Nakajima, Y. Honda, O. Kitao, H. Nakai, T. Vreven, K. Throssell, J. A. Montgomery, Jr., J. E. Peralta, F. Ogliaro, M. J. Bearpark, J. J. Heyd, E. N. Brothers, K. N. Kudin, V. N. Staroverov, T. A. Keith, R. Kobayashi, J. Normand, K. Raghavachari, A. P. Rendell, J. C. Burant, S. S. Iyengar, J. Tomasi, M. Cossi, J. M. Millam, M. Klene, C. Adamo, R. Cammi, J. W. Ochterski, R. L. Martin, K. Morokuma, O. Farkas, J. B. Foresman and D. J. Fox, *Gaussian 16, Revision B.01*, Gaussian, Inc., Wallingford CT, 2016.
56 V. Barone, *J. Chem. Phys.*, 2005, **122**, 014108.
57 J. Bloino and V. Barone, *J. Chem. Phys.*, 2012, **136**, 124108.
58 G. A. Zhurko, ChemCraft, Version 1.8. http://www.chemcraftprog.com, 2016, last accessed April 26, 2019.
59 S. Grimme, *J. Chem. Phys.*, 2006, **124**, 034108.
60 A. D. Becke, *J. Chem. Phys.*, 1993, **98**, 5648–5652.
61 C. Lee, W. Yang and R. G. Parr, *Phys. Rev. B: Condens. Matter Mater. Phys.*, 1988, **37**, 785–789.
62 F. A. Hamprecht, A. J. Cohen, D. J. Tozer and N. C. Handy, *J. Chem. Phys.*, 1998, **109**, 6264–6271.
63 C. Adamo and V. Barone, *J. Chem. Phys.*, 1999, **110**, 6158–6170.
64 V. Barone, P. Cimino and E. Stendardo, *J. Chem. Theory Comput.*, 2008, **4**, 751–764.
65 Double and triple-ζ basis sets of SNS, are available for download at https://smart.sns.it, accessed August 22, 2019.
66 R. Ditchfield, W. J. Hehre and J. A. Pople, *J. Chem. Phys.*, 1971, **54**, 724–728.
67 T. H. Dunning, *J. Chem. Phys.*, 1989, **90**, 1007–1023.
68 S. Grimme, J. Antony, S. Ehrlich and H. Krieg, *J. Chem. Phys.*, 2010, **132**, 154104.